ON THE CHARACTERIZATION OF SPRAYS PRODUCED BY WATER-MIST INJECTORS

Paolo E. Santangelo[a,1], Paolo Tartarini[a], André W. Marshall[b], Massimo Bettati[c]

[a] Dipartimento di Ingegneria Meccanica e Civile, Università degli Studi di Modena e Reggio Emilia, Modena, Italy

[b] Department of Fire Protection Engineering, University of Maryland, College Park, MD, USA

[c] Bettati Antincendio S.r.l., Reggio Emilia, Italy

Abstract

The present work is aimed at providing a thorough characterization of the spray produced by a water-mist injector. An experimental investigation on drop-size and flux distribution, initial velocity and spray-cone angle is proposed. These parameters appear to be the most suitable to provide a quantification of atomization and dispersion phenomena in any generic spray. In addition, some numerical simulations of the sprayed flow have been run employing FDS (Fire Dynamics Simulator): its capability of predicting the fluid-dynamics behavior of the spray has been challenged through a comparison with experimental outcomes. An experimental facility has been built to serve as the set for the entire experimental campaign. A typical water-mist nozzle has been inserted and the activity has been focused on one of the available injectors. Laser-based diagnostics has been employed to measure drop size and initial velocity. Most notably, a Fraunhofer-diffraction-based device (*Malvern Spraytec*) has been used to investigate the former, while the latter has been evaluated through PIV (Particle Image Velocimetry) technique. FDS code has been employed to carry out some simulations of the behavior of the water-mist spray. The implemented settings and initial conditions resulted from the experimental study, while the computational domain has been set to reproduce the test room. Then, numerical predictions have been validated through a comparison with experimental outcomes. In addition, a classic correlation to predict characteristic drop size has been proposed for the present case and validated.

Keywords: water mist, atomization, dispersion, laser-based techniques, numerical modeling

Introduction

Water-mist fire-suppression systems have become a promising technology in the fire-fighting field, especially since *halons* have been banned. They are now mainly employed for residential and industrial units, but even aeronautic and naval fields seem to be interested in them. As far as such systems are relatively new, strong efforts have been spent to perform research on them. Among all the works available in the open literature it is worth to mention the studies realized by the US Navy [1-3] to evaluate water mist performances for shipboard applications. Other fundamental analyses have been carried out by Lentati and Chelliah [4], Grant et al. [5] and Chelliah [6] in order to investigate physical phenomena occurring in fire suppression with water mist. Most of the works [1-4,6-8] are focused on suppression mechanism and fluid-flame interaction: several studies were aimed at analyzing suppression performances, but only limited researches [5] have been conducted to investigate sprays in these systems. Transport phenomena in water-mist sprays are generally characterized by high pressure injection (> 35 bar) and relatively small drops (characteristic diameter D_{v50} lower than 100 μm). The real advantage of these two features is the capability of spreading water droplets over a large area, while difficulties arise in interacting with fire and in overtaking potential obstructions. Transport and suppression depend on atomization and dispersion characteristics of spray. This work is aimed at investigating drop size and initial velocity at high operative pressures (> 50 bar). High values of pressure seem to be particularly interesting for the market because of the high-suppression effectiveness they provide. High-pressure sprays have been largely investigated for several applications and different fluids. Among the others, Yule and Widger [9] have studied water sprays produced by swirl atomizers, Senecal et al. [10] the linear stability of a high speed viscous liquid sheet and Sovani et al. [11] the effect of ambient pressure on spray cone angle.

A typical high pressure water mist nozzle has been employed in order to perform the experimental campaign. This nozzle typology is commonly used also in gas turbine field [12] in order to realize the cooling effect produced by water fog on turbine blades. Drop size is a parameter of interest to analyze sprays and many efforts have been spent in order to determine it both experimentally and theoretically. Among the several studies on this subject, it is worthwhile to mention the works performed by Lorenzetto and Lefebvre [13] about plain jet atomizers and by Yule et al. [14] about vaporizing sprays. Drop-size measurements have been carried out using

---

a laser-based device, the *Malvern Spraytec*. This has also been employed by Chaker et al. [12] to measure drop size in gas-turbine fogging and by Santangelo et al. [15], while Zhu and Chigier [16] have discussed a method to process data related to sprays. Mass-flux distribution has been determined using a mechanical patternator. Patternation measurements in sprays have already been mentioned by Sovani et al. [17] because of the necessity of having a quantitative feedback about dispersion.

Many atomization correlations have been developed to evaluate the characteristic size of droplets. These engineering correlations are summarized in [18], but they are mainly related to different applications (internal combustion engines, in particular) and to different fluids (gasoline, kerosene or fuels in general). Their validation for water mist systems is one of the aims of this study. To this end, a theoretical model has been developed following the one proposed in [18] about pressure swirl atomizers and, finally, a correlation has been validated showing promising results.

Initial velocity of the spray has been investigated and determined by Particle Image Velocimetry (PIV). This technique is now largely employed in fluid dynamics, but it has rarely been applied to the particular field of the present study. Widmann et al. [19] and Sheppard [20] have performed PIV tests on traditional sprinkler sprays, while Presser et al. [21] have studied the water mist flow over different kinds of obstacle. Basic works have been performed by Bachalo [22] describing PIV as one of the experimental methods in multiphase flows, by Ikeda et al. [23] and Palero and Ikeda [24] applying uncertainty analysis and drop-size-based discrimination to study turbulence of a spray. The primary purpose of this investigation is to determine the initial velocity of the spray and its gap with respect to the one obtained from the physical analysis. Moreover, an evaluation of the spray-cone angle has been stressed out from the PIV maps. It is worthwhile to mention two comprehensive doctoral works performed by Paulsen Husted [25] and Santangelo [26], where a thorough experimental approach to water-mist sprays is developed and applied.

Numerical analyses of water-mist systems have been conducted over many applications [27-30], especially employing FDS (Fire Dynamics Simulator). However, the numerical approach has been mainly focused on predicting the flow-flame interaction, that practically means the suppression performance. Therefore, this work has been carried out to understand the code capability of properly simulating a water-mist spray. To this end, the already mentioned parameters have been set as the input and the measured volume-flux distribution has been employed as the validating tool.

Experimental setup and results

An experimental facility has been built to perform all the mentioned measurements. The nozzle (Fig. 1a, no. 1) has been placed at 2 m height from the floor. This nozzle is constituted by 6 peripheral injectors and the central one: tests have been carried out on the spray produced by this latter. A tank (Fig. 1a, no. 2), an electric pump (Fig. 1a, no. 3) and a pressure gauge (Fig. 1a, no. 4) have been conveniently installed. A *Malvern Spraytec* device (Fig. 1a, no. 5) has been adjusted in order to have the laser beam at 1 m height from the floor. The PIV system consists of a laser emitter (pulsed 30 mJ Nd:YAG) and a thermo-electrically cooled CCD camera (14 bit, 4 Mpx). The laser emitter (Fig. 1a and 1b, no. 6) and the camera (Fig. 1b, no. 8) have been set to illuminate the initial region of the spray and to take images of the sampling area with no angular correction. Velocity maps have been reconstructed averaging a set of 300 double images. A data acquisition system has been provided (Fig. 1a and 1b, no. 7). Volume-flux distribution has been measured through a home made mechanical patternator (Fig. 1b, no. 9).
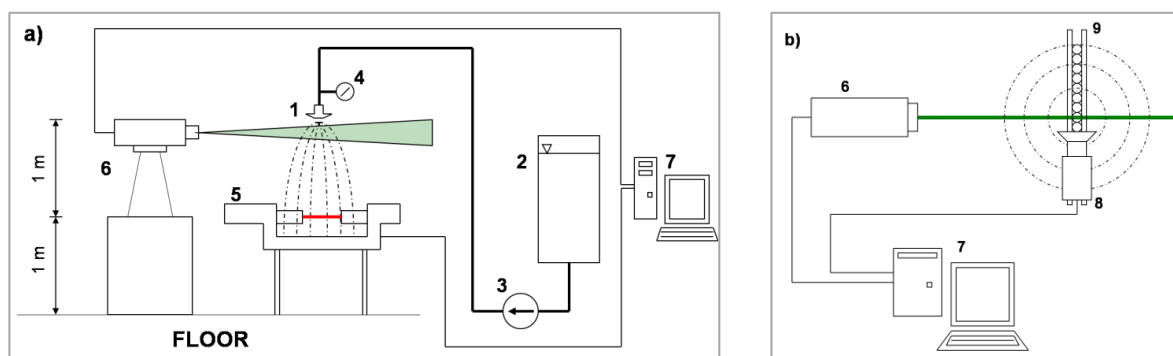
Fig. 1 Sketch of the experimental facility: a) view from side (*Malvern Spraytec* and PIV system); b) view from above (PIV system and mechanical patternator).

It is constituted by a set of 55 plastic tubes. The inlet section of every tube has been made perpendicular to the injector axis. The frame of the patternator has been adjusted to collect water at 1 m height from the floor: therefore, drop-size and volume-flux measurements are performed over the same spray cross section. The central tube has been placed right under the injector, so its axis was coincident with the injector one. The

experimental campaign has been carried out to cover the already mentioned range of high operative pressure: tests have been run at 60, 70 and 80 bar. Operative pressure means the value reported by the pressure gauge, that practically represents the pressure right upstream the nozzle.

An experimental methodology has been developed to gain a proper evaluation of the numerous parameters. An extensive description of any proposed procedure is presented in Santangelo et al. [15,30] and Santangelo [26]. However, it is worthwhile to briefly summarize the main points. Drop-size measurements have been taken by the *Malvern Spraytec* at a prescribed number of radial locations, being this analysis based on hypothesis of symmetry for any spray cross section. Then volume-flux distribution has been measured by the mechanical patternator, that has been placed along a diameter of the spray cross section. Hypothesis of diametrical symmetry has been applied. A center of volume flux has been calculated for each test: this point has been identified as the real center and it is not perfectly coincident with the intersection between the injector axis and the spray cross section, due to little experimental asymmetries. Finally, a curve of volume-flux distribution has been extrapolated to express this parameter as a function of the radial coordinate. Drop-size distribution has been reconstructed by weighting drop-size measurements through volume-flux distribution. This procedure allows to obtain a proper evaluation of drop-size distribution as a result of an averaging process through another parameter (volume flux) and not only as a simple measurements by the *Malvern Spraytec*. A typical Rosin-Rammler log-normal distribution has been employed to predict the drop-size trend as a function of the volume fraction. This distribution is expressed as:

$$CVF = \begin{cases} (2\pi)^{-1/2} \int_0^{D_{CVF}} (\gamma' D)^{-1} e^{-\frac{[\ln(D/D_{v50})]^2}{2\gamma'^2}} \, dD & (D_{CVF} \leq D_{v50}), \\ 1 - e^{-0.693(D_{CVF}/D_{v50})^\gamma} & (D_{v50} < D_{CVF}), \end{cases} \tag{1}$$

where D is the generic droplet diameter, CVF is the Cumulative Volume Fraction, γ is a curve-fitting coefficient and γ' is expressed as $\gamma' = 2((2\pi)^{1/2}(\ln 2)\gamma)^{-1}$. Suitable values for the curve-fitting γ coefficient have been determined to gain the best agreement between the experimental drop-size trend and the predictive function. As an example, Fig. 2 reports the averaged volume-flux distribution at every value of operative pressure, while Fig. 3 shows the reconstructed drop-size distribution at 80 bar of operative pressure. As a summary of the experimental results on drop size, Fig. 4 reports the trend of SMD and D_{v50} with respect to operative pressure; moreover, Fig. 4 also shows the γ coefficient as a function of pressure: it appears to be almost constant over the range of interest.
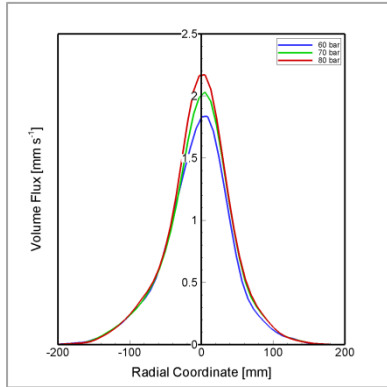
Fig. 2 Average volume-flux distribution.
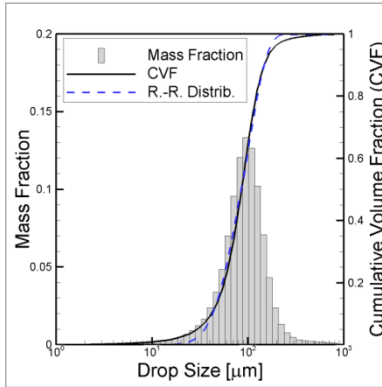
Fig. 3 Drop Size vs. Cumulative Volume Fraction.
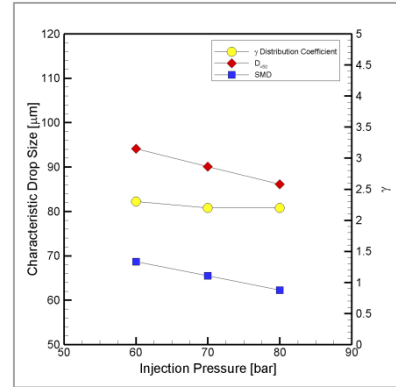
Fig. 4 D_{v50}, SMD and γ coefficient vs. Operative Pressure.

The PIV experimental campaign has been carried out without any seeding, because water droplets produced by a pressure-swirl atomizer at high pressure are tiny enough to be tracking particles themselves. However, reliable values of velocity were practically obtained as of a distance of about 2 mm from the injector outlet along the axis. As an example, Fig. 5 shows the reconstructed PIV map at 80 bar, while Fig. 6 reports the trend of non-dimensional initial velocity. This latter value derives from the ratio between the initial velocity magnitude and a reference value resulting from a Bernoulli model (see Eq. (2)):

$$V = \sqrt{\frac{2p_{PG}}{\rho_L}}, \tag{2}$$

where V is the reference velocity at the injector outlet, p_{PG} is the value measured by the pressure gauge and ρ_L is the density of the liquid phase (water). The velocity measurements have taken into account radial and axial

components. Two-dimensional measurements of a three-dimensional vectorial parameter are based on the physical approximation that tangential component tends to become negligible once the flow leaves the injector. Angular velocity tends to decrease very fast once the generic particle (droplet) has been produced: thus, the tangential component can be neglected after a short axial distance from the injector outlet (around 5 mm). Velocity profiles have also been employed to determine the spray-cone angle and its trend along the axial extension of the PIV sampling area. As a final outcome of the PIV campaign, an evaluation of the spray-cone angle has been stressed out through a simple geometric procedure applied to velocity profiles at different distances from the injector outlet. Fig. 7 shows its trend moving downwards from the orifice: sub-regions 0, 1 and 2 identify a sub-division of the PIV sampling area from the outlet through its lower limit.
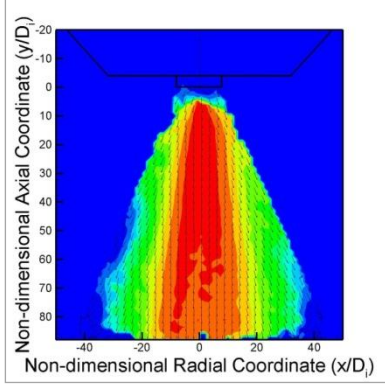
Fig. 5 PIV maps (vectors and contours).	**Fig. 6** Initial non-dimensional velocity magnitude.	**Fig. 7** Trend of spray-cone angle.
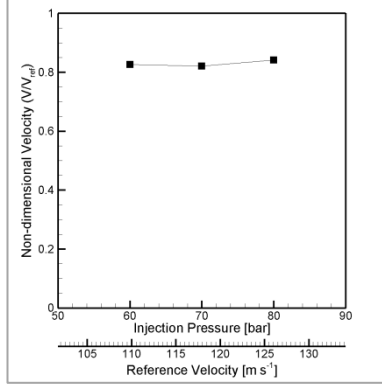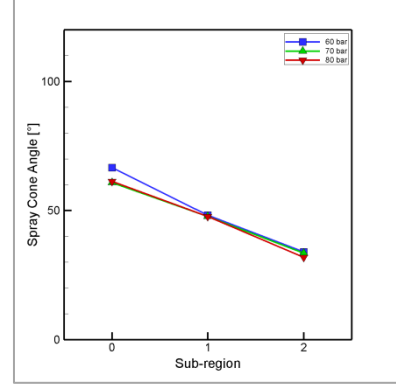
A strong stream in the central region of the spray shows high velocity magnitude (Fig. 5): its motion appears to be momentum-driven and is governed by the imposed static load (operative pressure). On the other hand, particles located in the peripheral regions are characterized by low velocity magnitude. Therefore, they basically float within the surrounding fluid, being their motion buoyancy-driven. The initial non-dimensional velocity (Fig. 6) appears to be almost constant as operative pressure varies: its value is slightly above 80%. Therefore, the reference value given by Eq. (2) may be of interest as an input for numerical models, being the relative error lower than 20% over the considered pressure range. The spray-cone angle does not appear to be remarkably affected by the operative pressure, while it tends to decrease as the distance from the orifice increases. This outcome is consistent with the classic theory about pressure-swirl atomizers, clearly described by Lefebvre [18]: the spray tends to be constrained by the interactions with the surrounding fluid, so the cone angle decreases moving downwards along the axial coordinate.

Physical analysis: characteristic drop-size correlation

A theoretical approach has been developed to validate a predictive formula for the characteristic diameter of the spray. A schematic geometry of the injector (Fig. 8) has been adopted to apply a physical approach. Water flows with straight motion between sections 0 and 1: this the injector slot and it is sloped at an angle ϕ with respect to the axis. The path between sections 1 and 2 (outlet) is the swirl chamber: it is basically a convergent-divergent duct, showing a final inclination of θ with respect to the axis. Following the discussion proposed by Lefebvre [18] about pressure-swirl atomizers, a Bernoulli equation has been introduced:

$$P = p_1 - p_{atm} + \frac{1}{2}\rho_L V_1^2 = p_2 - p_{atm} + \frac{1}{2}\rho_L V_2^2, \tag{3}$$

where P is the total pressure, p is the static pressure, *atm* stands for atmospheric, *1* and *2* refer to the corresponding sections. As far as the assumption of inviscid fluid has been implicitly stated, total pressure is constant along the path 0-2. This pressure may be measured by a Pitot tube at any location of the path, but a pressure gauge has been installed at section 0. Since dynamic load at section 0 is considered to be negligible, the value measured by the pressure gauge is assumed to be representative of total pressure, yielding Eq. (2).

The definition of the discharge coefficient is commonly adopted in the internal-combustion-engine field. This coefficient can be used for any kind of nozzle or injector and represents the ratio between the effective area of fluid transit and the geometric cross section of the orifice:

$$C_D = \frac{A_F}{A_{TOT}}, \qquad C_D \in [0,1]. \tag{4}$$

An expression for mass flow rate can be easily obtained from Eqs. (2) and (4):

$$\dot{m}_L = \rho_L A_F V_2 = \rho_L C_D A_{TOT} V_2 = C_D A_{TOT} \sqrt{2\rho_L p_{PG}}. \tag{5}$$

The crucial point is to determine the discharge coefficient, because the other parameters have been either *a priori* known (area of the outlet), or measured (pressure), or detected from technical tables (density). To this end an additional parameter should be introduced: the flow number, commonly used in the water-mist field and known as a design parameter. The relation between flow number and discharge coefficient is the key to gain this latter and finally the mass flow rate:

$$C_D = \frac{FN}{A_{TOT}} \sqrt{\frac{\rho_L}{2}}. \tag{6}$$

Mass flow rate has been calculated as a result of the described procedure. As the last step, a correlation has been validated to predict the characteristic drop size of the spray. Many correlation are available in the scientific literature about high-pressure sprays, being mainly developed for fuels (gasoline, kerosene, etc.) rather than other fluids, as results of studies in the combustion-engine or gas-turbine field. In particular, the classic correlation proposed by Radcliffe [26] has shown promising agreement for water-mist sprays:

$$SMD = 7.3 \cdot \sigma^{0.6} \cdot \nu^{0.2} \cdot \dot{m}_L^{0.25} \cdot p_L^{-0.4}, \tag{7}$$

where σ is the surface tension and ν is the kinematic viscosity of the sprayed fluid. Fig. 9 shows the trend of experimental and predicted SMD as a function of operative pressure.
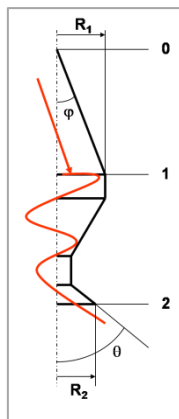
Fig. 8 Qualitative sketch of the flow within the injector.
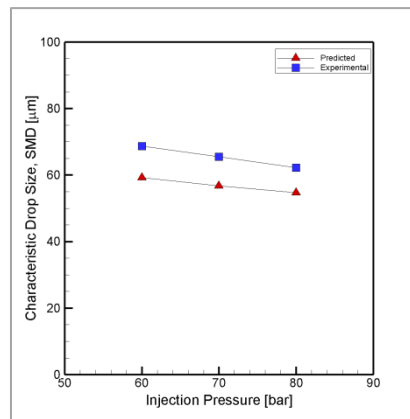
Fig. 9 Comparison between experimental and predicted SMD over the considered pressure range.

The validated correlation tends to underestimate the SMD with a relative error lower than 15%. Moreover, the trends of experimental and predicted SMD are very consistent one to the other.

Numerical modeling

Some numerical simulations have been carried out to challenge well recognized code in reproducing the dynamic behavior of a water-mist spray. FDS (Fire Dynamics Simulator) and Fluent® have been chosen as the computational codes to the purpose. The former is a well established resource for numerical simulations of fire scenarios. However, it has been mainly developed for traditional-sprinkler sprays and its predictability about high-pressure and high-velocity sprays like water mist has to be explored. Fluent® is a well known code for general applications in fluid dynamics, but it also has to be challenged in simulating dispersed flows like this one. The test room has been modeled as the physical domain in both the codes and almost the same initial conditions have been implemented from the experimental campaign.

FDS solves a form of the Navier-Stokes equations appropriate for low-speed thermally-driven flows. Partial derivatives of mass, momentum and energy-conservation equations are approximated as finite differences, and the solution is updated in time on a three-dimensional, rectilinear grid. Turbulence can be modeled either through Large Eddy Simulation (LES) or Direct Numerical Simulation (DNS). LES appears to be the most appealing approach to investigate large-scale applications, like this one. This technique is based on a direct model of transient large eddies, while eddies smaller than the grid scale are treated by a Smagorinsky form. In addition, FDS employs the Euler-Lagrangian method to model the particle transport. By this approach,

trajectories of a representative number of droplets are predicted and momentum is transferred between the two phases (liquid and gaseous) applying the particle-source-in-cell method. FDS does not provide a physical simulation of droplet collision and break-up phenomenon. However, a semi-empirical model is introduced to simulate the droplet evaporation.

Some simulations employing FDS 5.2 have been performed. A rectangular computational domain was set with dimensions of 1.0 m (x) by 1.0 m (y) and 2.0 m (z) height in a Cartesian coordinate. The injector has been set on the top of the z domain and centered on the x-y axes. The geometry was divided into 11 grids, which become coarser moving downwards from the injector. All the boundaries of the geometry have been set as open vents except for the floor, that has been identified as a close surface. The droplets have been inserted 10 mm below the nozzle with the measured velocities. Furthermore, 30000 droplets per second have been released at intervals of 4.5 ms to model the water spray. The results of numerical simulations of the droplet volume flux at 1 m below the nozzle are reported for three different operative pressures (60, 70 and 80 bar) and are compared with the related experimental data (Fig. 10). The predicted values are about two times greater than the measured ones. In terms of discrepancy between numerical and experimental results, FDS appears to overestimate the volume flux in a 40 mm radius from the centre (perpendicular to the injector) and then starts to underestimate the flux. The experimental peak at 70 bar is perfectly amid the ones at 60 bar and at 80 bar on experimental curves, while this trend is not exactly reproduced by FDS. As a matter of fact, the calculated values at 70 bar are closer to the ones computed at 80 bar in the numerical simulation.

Very few works are available in the open literature about Fluent[®] applied to water mist, even because this code is not usually employed in fire-protection field. The two-phase models implemented in Fluent[®] have been validated by comparing volume-flux distribution numerically obtained with experimental data. Two different methods may be used to face a water-mist case: the Discrete Phase (DP) and the Eulerian Species Transport (EST) models. The EST model in Fluent allows to model multiple separate interacting phases. Phases can be liquid, gas, or solid in almost any combination. A Eulerian approach is used for each phase, in contrast with the Eulerian-Lagrangian approach that is used for the DP model. The description of multiphase flow as interpenetrating continua incorporates the concept of phasic volume fractions. Volume fractions represent the space occupied by each phase and mass and momentum-conservation laws are obeyed by each phase individually. Derivation of conservation equations is performed by averaging the local instantaneous balance for each of the phases or by using the mixture-theory approach. The same k-ε model simulating turbulence within the fluid phase in DP approach has been used to describe both phases in EST approach. As expectable, only the EST model has been employed, as far as the available literature shows that it is the most appropriate for dense and tiny water droplets. The geometry and the mesh have been generated using Gambit pre-processor, provided by Fluent[®] package. A volume with the same dimensions of the injector has been built and the production of droplets has been modeled as a mass-source term in correspondence to this volume. The geometry of the rest of the domain is a cube 2.0 m by 2.0 m by 2.0 m. Wall boundary conditions have been set at top and floor surfaces of this domain, while symmetric boundary conditions have been set at the lateral surfaces of the computational domain. The simulations are not capable of getting collision and coalescence of droplets, collapse of the spray and momentum transfer from droplets to air. This approach leads to overestimate dimensions of the spray cone with respect to experimental results as well as droplet velocity distribution.

Fig. 11 shows a comparison between droplet volume flux obtained by Fluent[®] under the second approach at a distance of 1 m from the injector outlet.
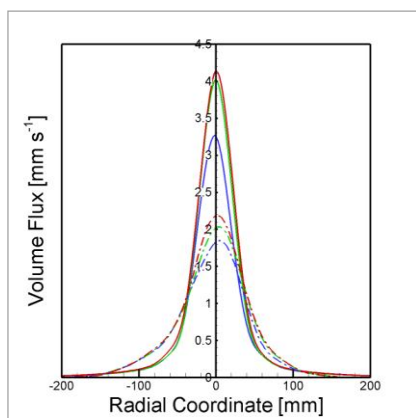
Fig. 10 Comparison between experimental (dashed-dot) and FDS numerical (solid) volume-flux curves at 60 (blue), 70 (green) and 80 (red) bar.
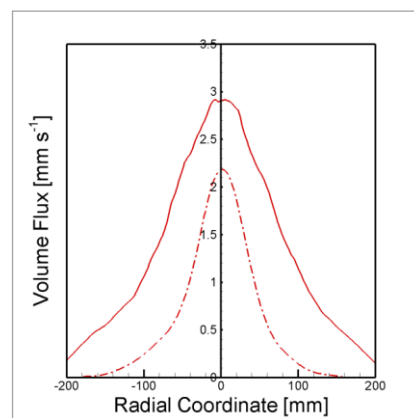
Fig. 11 Comparison between experimental (dashed-dot) and Fluent[®] numerical (solid) volume-flux curves.

A reasonable qualitative agreement between numerical and experimental data is stressed out, even if the computational code tends to generally overestimate this parameter. As far as this computational analysis by Fluent® represents a preliminary attempt, only the operative pressure of 80 bar has been considered in the numerical simulations.

Conclusions

A thorough characterization of water-mist sprays operating at high pressure has been performed in terms of atomization and dispersion. Most notably, laser-based techniques have been employed to experimentally determine drop-size distribution, velocity field (magnitude and vectors) and spray-cone angle. In addition, flux distribution has been evaluated through a mechanical patternator. Suitable methodologies have been developed to post-process the experimental data and finally reconstruct the appropriate trend of velocity and drop-size distribution. A classic correlation to predict the SMD over the considered range of operative pressure has been proposed and validated for the present case as a final result of a physical analysis. Some numerical simulations have been carried out employing FDS and Fluent®: to this end, some efforts have been spent on modeling the water-mist flow. The computational approach was aimed at validating these computational codes in terms of dynamic behavior of the spray. Volume-flux distribution has been identified as the key parameter for the comparison. FDS yielded a qualitatively good agreement with the experimental data, even if spray penetration appears to not be thoroughly modeled; therefore, the central peak is overestimated, whereas an underestimation occurs in the peripheral diametrical regions. On the other hand, Fluent® has produced a general overestimation, that might be due to an imperfect evaluation of the immediate evaporation of the tiniest droplets.

References

[1] C.C. Ndubizu, R. Ananth, P.A. Tatem and V. Motevalli, On water mist fire suppression mechanisms in a gaseous diffusion flame, *Fire Saf. J.*, vol. 31, pp. 253-276, 1998.

[2] K.C. Adiga, R.F. Hatcher Jr., R.S. Sheinson, F.W. Williams and S. Ayers, A computational and experimental study of ultra fine water mist as a total flooding agent, *Fire Saf. J.*, vol. 42, pp. 150-160, 2007.

[3] B.T. Fisher, A.R. Awtry, R.S. Sheinson and J.W. Fleming, Flow behavior impact on the suppression effectiveness of sub-10-µm water drops in propane/air co-flow non-premixed flames, *Proc. Combust. Inst.*, vol. 31, pp. 2731-2739, 2007.

[4] A.M. Lentati and H.K. Chelliah, Dynamics of water droplets in a counterflow field and their effect on flame extinction, *Combust. Flame*, vol. 115, pp. 158-179, 1998.

[5] G. Grant, J. Brenton and D. Drysdale, Fire suppression by water sprays, *Prog. Energ. Combust. Sci.*, vol. 26, pp. 79-130, 2000.

[6] H.K. Chelliah, Flame inhibition/suppression by water mist: droplet size/surface area, flame structure, and flow residence time effects, *Proc. Combust. Inst.*, vol. 31, pp. 2711-2719, 2007.

[7] G.O. Thomas, The quenching of laminar methane-air flames by water mists, *Combust. Flame*, vol. 130, pp. 147-160, 2002.

[8] T. Parra, F. Castro, C. Méndez, J.M. Villafruela and M.A. Rodríguez, Extinction of premixed methane-air flames by water mist, *Fire Saf. J.*, vol. 39, pp. 581-600, 2004.

[9] A.J. Yule and I.R. Widger, Swirl atomizers operating at high water pressure, *Int. J. Mech. Sci.*, vol. 38, pp. 981-999, 1996.

[10] P.K. Senecal, D.P. Schmidt, I. Nouar, C.J. Rutland, R.D. Reitz and M.L. Corradini, Modeling high-speed viscous liquid sheet atomization, *Int. J. Multiph. Flow*, vol. 25, pp. 1073-1097, 1999.

[11] S.D. Sovani, E. Chou, P.E. Sojka, J.P. Gore, W.A. Eckerle and J.D. Crofts, High pressure effervescent atomization: effect of ambient pressure on spray cone angle, *Fuel*, vol. 80, pp. 427-435, 2001.

[12] M. Chaker, C.B. Meher-Homji and T. Mee III, Inlet fogging of gas turbine engines – Part II: Fog droplet sizing analysis, nozzle types, measurements, and testing, *J. Eng. Gas Turbines Power – Trans. ASME*, vol. 126, pp. 559-570, 2004.

[13] G.E. Lorenzetto and A.H. Lefebvre, Measurements of drop size on a plain jet airblast atomizer, *AIAA J.*, vol. 15, pp. 1006-1010, 1977.

[14] A.J. Yule, P.R. Ereaut and A. Ungut, Droplet sizes and velocities in vaporizing sprays, *Combust. Flame*, vol. 54, pp. 15-22, 1983.

[15] P.E. Santangelo, N. Ren, P. Tartarini and A.W. Marshall, Spray characterization of high pressure water mist injectors: experimental and theoretical analysis, *Proc. of Twenty-second European Conference on Liquid Atomization and Spray Systems – ILASS 2008*, Como Lake, Italy, 2008, paper 10-5.

[16] H.M. Zhu and N. Chigier, Tomographical transformation of Malvern measurements, *Int. Commun. Heat Mass Transf.*, vol. 13, pp. 483-491, 1986.

[17] S.D. Sovani, P.E. Sojka and A.H. Lefebvre, Effervescent atomization, *Prog. Energy Combust. Sci.*, vol. 27, pp. 483-521, 2001.

[18] A.H. Lefebvre, Atomization and Sprays, Hemisphere, New York City, NY, USA, 1989.

[19] J.F. Widmann, D.T. Sheppard and R.M. Lueptow, Non-Intrusive Measurements in Fire Sprinkler Sprays, *Fire Technol.*, vol. 37, pp. 297-315, 2001.

[20] D.T. Sheppard, Spray Characteristics of Fire Sprinklers, Ph.D. thesis, Northwestern University, Evanston, IL, USA, 2002.

[21] C. Presser, G. Papadopoulos and J.F. Widmann, PIV measurements of water mist transport in a homogeneous turbulent flow past an obstacle, *Fire Saf. J.*, vol. 41, pp. 580-604, 2006.

[22] W.D. Bachalo, Experimental methods in multiphase flows, *Int. J. Multiph. Flow*, vol. 20, pp. 261-295, 1994.

[23] Y. Ikeda, N. Yamada and T. Nakajima, Multi-intensity-layer particle-image velocimetry for spray measurement, *Meas. Sci. Technol.*, vol. 11, pp. 617-626, 2000.

[24] V.R. Palero and Y. Ikeda, Droplet-size-classified stereoscopic PIV for spray characterization, *Meas. Sci. Technol.*, vol. 13, pp. 1050-1057, 2002.

[25] B. Paulsen Husted, Experimental measurements of water mist systems and implications for modelling in CFD, Doctoral thesis, Lund University, Lund, Sweden, 2007.

[26] P.E. Santangelo, Characterization of water-mist sprays: experimental and theoretical analysis of atomization and dispersion, Doctoral thesis, Università degli Studi di Modena e Reggio Emilia, Modena, Italy, 2009

[27] S.C. Kim and H.S. Ryou, An experimental and numerical study on fire suppression using a water mist in an enclosure, *Build. Environ.*, vol. 38, pp. 1309-1316, 2003.

[28] S. Hostikka and K. McGrattan, Numerical modeling of radiative heat transfer in water sprays, *Fire Saf. J.*, vol. 41, pp. 76-86, 2006.

[29] C.L. Shi, W.Z. Lu, W.K. Chow, and R. Huo, An investigation on spill plume development and natural filling in large full-scale atrium under retail shop fire, *Int. J. Heat Mass Transf.*, vol. 50, pp. 513-529, 2007.

[30] P.E. Santangelo, P. Tartarini, B. Pulviranti and P. Valdiserri, Discharge and Dispersion in Water-Mist sprays: Experimental and Numerical Analysis, in *Proc. of 11th Triennial International Conference on Liquid Atomization and Spray Systems - ICLASS 2009*, Vail, CO, USA, 2009, paper 051.